

Optimal configuration of dual-arm cam-lock robot based on task-space manipulability

Kambiz Ghaemi Osgouie*, Ali Meghdari* and Saeed Sohrabpour

*Center of Excellence in Design, Robotics and Automation, Sharif University of Technology, 11365-9567, Tehran (IRAN).
E-mail: osgouie@mech.sharif.edu, sohrabpour@sharif.edu*

(Received in Final Form: February 16, 2008. First published online: April 11, 2008)

SUMMARY

In this paper obtaining the optimal configuration of the dual-arm cam-lock (DACL) robot at a specific point is addressed. The objective is to optimize the applicable task-space force in a desired direction. The DACL robot is a reconfigurable manipulator formed by two parallel cooperative arms. The arms normally operate redundantly but when needed, they can lock into each other in certain joints in order to achieve a higher stiffness, while losing some degrees of freedom. Furthermore, the dynamics of the DACL robot is discussed and parametrically formulated. Considering the geometrical constraints at a given point in the robot's workspace, the optimum configuration for maximizing the cooperatively applicable force by dual arms is determined.

KEYWORDS: Dual-arm Robot; Dynamic Optimization; Manipulator Optimization; Adaptive Configuration.

1. Introduction

Cooperative robot systems have been receiving increasing attention from the robotics research community. They are believed to offer enhanced capabilities over current single-arm structures. Nonetheless, this research field covers the interesting case of multi-fingered robot hands, in which the same kind of issues are encountered.¹ A cooperative strategy with two arms is necessary to perform all those tasks that cannot be easily executed by a single-arm robot. Typical cooperation examples include tasks such as handling large, heavy, or non-rigid objects; assembly and mating of mechanical parts; and space robotic applications.

In spite of the potential benefits of multiple-arm robots, analysis and control of such mechanisms is a complex issue, which is due to the kinematic and dynamic interactions imposed by cooperation. This means that in the tasks requiring effective cooperation, extension of the well-known results for the kinematics, dynamics, and control of single-arm robots is not straightforward. Therefore, for solving such problems, a global description of a multi-arm system is needed.

Referring to the simple case of a two-arm system, two main approaches have been proposed in literature: the master-slave strategy, and the task-space oriented formulation. The former consists of defining the desired motion of the object to be manipulated, while deriving the motion for the follower

arm using the set of holonomic constraints determined by the closed chain system.² The latter strategy has been shown to be more effective for coordinated control schemes, with equal importance given to the two robots performing the given task.³ In this method, a suitable set of static global task-space coordinates is defined in terms of absolute generalized forces between the two end-effectors. Then, based on the duality principle between kinematics and statics, global task-space kinematic coordinates are derived. The coordinates describe the absolute velocities of the object and the velocities of the two end-effectors relative to each other. This formulation can be formally extended to the case of multiple-arm systems as it is shown in ref. [3]. In particular, internal forces are defined at object level, which is different from the method presented in ref. [4], where they are represented at the end-effector level. In this scenario, an important issue is to define the quantitative measures of performance offered by multi-arm cooperation.

The velocity and force manipulability ellipsoids introduced in ref. [5] are widely adopted as kinetostatic performance indices for a single arm. These are not absolute numerical measures of robot system capabilities, which are independent of the physical force/velocity limitations. In other words, the ellipsoids do not give the maximum force/velocity along different task directions, and only indicate the preferred directions for the structures to perform force/velocity in a given configuration. This method was revised by Chiu⁶ and the manipulator was effectively regarded as a mechanical transformer of velocities and forces from the joint space to the task-space.

A dual-arm velocity manipulability ellipsoid is defined in ref. [7] as the maximum ellipsoid is determined by the intersection of the two single-arm velocity manipulability ellipsoids. The case to lose cooperation is also treated in ref. [7]. In this work, relative velocity and external plus internal force effects are not investigated, although they are important for the analysis of cooperation performance. In addition, only the dual-arm case is addressed, and the extension to the multi-arm case does not seem to be straightforward. An alternative approach has been proposed in ref. [8] based on the use of polytopes that properly account for the physical limits on the joint actuators. Although the method is technically correct, its practical application is limited due to the lack of a closed-form algorithm to derive the polytope in non-trivial cases.

Formal definitions of force and velocity manipulability ellipsoids for multiple cooperative arms are expressed in

* Corresponding author. E-mail: meghdari@sharif.edu

ref. [9]. These definitions are given in accordance with the above global task-space formulation that regards the closed chain system as a whole at the object level, and independent of the number of arms involved in the cooperation. For a given force/velocity task, the focus is on the evaluation of arms behaviour, rather than computing the actual physical limits of the multi-arm system.

Kim and Yoon¹⁰ have proposed two performance indices to quantify the dynamic responsiveness of a multi-arm robot as: the isotropic velocity radius (IVR) and the isotropic acceleration radius (IAR). They have developed an algorithm to obtain some concise explicit expressions for isotropic acceleration and velocity radii, without using the pseudo-inverse method.

In their recent paper, Krut *et al.*¹¹ have comprehensively discussed kinematic performance indices applied to parallel mechanisms having actuation redundancy. They have used both ellipsoid and polytope of velocity, and have employed singular value decomposition to investigate the kinematic isotropy of the mechanisms.¹² Also, Lau and Arteaga¹³ have recently investigated the dynamic model of a cooperative system consisting of two industrial robots, carrying a rigid object. The authors have developed kinematic and dynamic models of the system, considering some holonomic constraints to maintain the cooperative manipulation of the two arms.

In the present paper, the DACL robot is considered.¹⁴ This robot has two arms with joints able to lock into each other through a novel design. When some joints are locked, the robot loses some degrees of freedom, but meanwhile the arms gain improved stiffness. The concept of this manipulator is described further in Section 2. When different joints are locked into each other, the dynamics of the robot changes and one must assess which configuration of the robot is most suitable for the specified task. Here, we are interested in finding the best structure for the DACL robot, in which the manipulator is to exert maximum possible force in a specific point/direction in its dexterous workspace. The DACL robot considered here is composed of two 4-DOF planar arms. It is assumed that the closed-chain system grasps the object rigidly. Due to its redundant nature, the DACL robot may take various configurations when holding an object in a specific point in its “planar” workspace. Unlike other cooperative redundant arms currently considered in the literature, the DACL manipulator has the advantage of *locking joints* to improve its kinematic and dynamic performance.

2. The DACL Manipulator Concept

Without much exaggeration, one may claim that most of the suitable tasks in nature generally take place by the virtue of one or more dual or paired mechanisms. Natural motions of the human limbs and organs (hands, fingers, legs, eyes, ears, etc.) as well as wings of birds and the fins of fish, clearly indicate the importance of paired or dual mechanisms for an optimal performance. In situations where part of a pair is lost or is no longer functional, its importance becomes more and more evident.

In general terms, a dual-arm manipulator can be defined as a mechanism in which its elements are basically a mirror

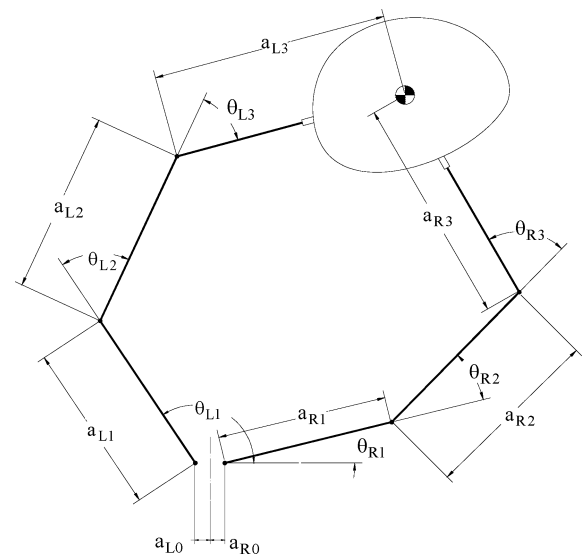


Fig. 1. Schematic of the dual-arm cam-lock robot with $n = 3$.

image of each other with respect to a predefined axis/plane of symmetry. A dual-arm manipulator is composed of two multi-link open-loop kinematic chains as shown schematically in Fig. 1, where $(\theta_{Ri}, a_{Ri}; i = 1, 2, \dots, n)$ and $(\theta_{Lj}, a_{Lj}; j = 1, 2, \dots, n)$ are the joint angles and the link lengths of the right and left manipulators, respectively (the figure is for $n = 3$).

As shown in Fig. 2, three general topologies may be considered for the manipulator. It can also possess a motion configuration in symmetric and nonsymmetric fashions with respect to a predefined axis of symmetry.

Figure 3 gives a brief description of one of the possible designs of the DACL robot. Its body is formed by a number of cams. Whenever needed, manipulator is able to lock some cams of the left and right sides together and thus gain a more rigid structure but of less degrees of freedom. Some applications and other configurations of the DACL manipulator are described in refs. [14–16].

3. Kinetostatics of the DACL Manipulator

Let us consider a DACL manipulator with each arm having four degrees-of-freedom ($n_R = n_L = 4$). The manipulator’s task-space is two-dimensional ($m = 2$) and a point object is to be held by the manipulator in the task-space. Figure 4

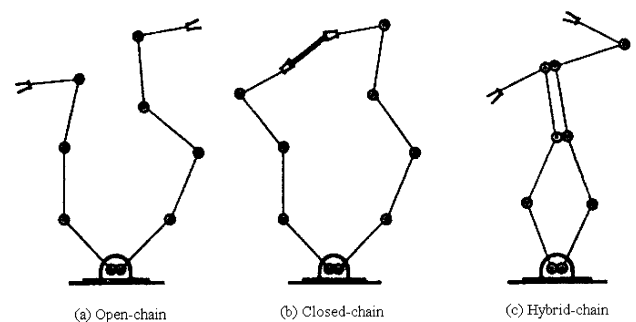


Fig. 2. Motion configurations of a dual-arm cam-lock robot with $n = 5$.

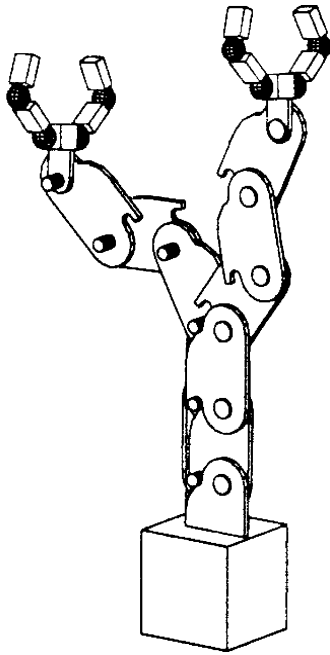


Fig. 3. A solid model of the dual-arm cam-lock robot.

shows the schematics of the manipulator and introduces the geometrical parameters of the arms. The object's position is measured in terms of the base coordinate system shown in the figure, and all angles are measured counter clockwise. Position of the tip point (i.e., the absolute coordinates of the object), in the base coordinate system $\{x_0, y_0\}$ is found as

$$\begin{aligned} P_x &= c_{R1234} \cdot a_{R4} + c_{R123} \cdot a_{R3} + c_{R12} \cdot a_{R2} + c_{R1} \cdot a_{R1} \\ P_y &= s_{R1234} \cdot a_{R4} + s_{R123} \cdot a_{R3} + s_{R12} \cdot a_{R2} + s_{R1} \cdot a_{R1} \end{aligned} \quad (1)$$

in which P_x and P_y are the object's location. Also $c_{R12..} = \cos(\theta_{R1} + \theta_{R2} + \dots)$ and $s_{R12..} = \sin(\theta_{R1} + \theta_{R2} + \dots)$. Note that (1) describes the tip point location in terms of the parameters of the right arm. Similarly, it can be described

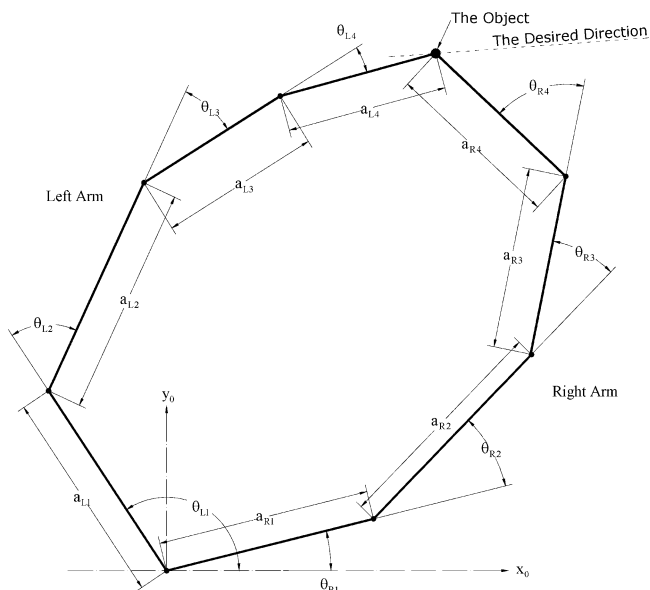


Fig. 4. Schematics of the DACL manipulator considered here.

by the parameters of the left arm

$$\begin{aligned} P_x &= c_{L1234} \cdot a_{L4} + c_{L123} \cdot a_{L3} + c_{L12} \cdot a_{L2} + c_{L1} \cdot a_{L1} \\ P_y &= s_{L1234} \cdot a_{L4} + s_{L123} \cdot a_{L3} + s_{L12} \cdot a_{L2} + s_{L1} \cdot a_{L1}. \end{aligned} \quad (2)$$

Thus, the four constraints that limit the motion of the arms in their individual workspaces are found. Note that grasping the object is such that only two degrees-of-freedom is specified for it (i.e., its rotation is not considered here).

By differentiating tip point's coordinates with respect to time and separating the angular velocities of the joints, the Jacobian matrix of the right arm can be found as

$$J_R = \begin{bmatrix} J_{R1,1} & J_{R1,2} & J_{R1,3} & J_{R1,4} \\ J_{R2,1} & J_{R2,2} & J_{R2,3} & J_{R2,4} \end{bmatrix}, \quad (3)$$

in which

$$\begin{aligned} J_{R1,1} &= -s_{R1234} \cdot a_{R4} - s_{R123} \cdot a_{R3} - s_{R12} \cdot a_{R2} - s_{R1} \cdot a_{R1} \\ J_{R1,2} &= -s_{R1234} \cdot a_{R4} - s_{R123} \cdot a_{R3} - s_{R12} \cdot a_{R2} \\ J_{R1,3} &= -s_{R1234} \cdot a_{R4} - s_{R123} \cdot a_{R3} \\ J_{R1,4} &= -s_{R1234} \cdot a_{R4} \\ J_{R2,1} &= c_{R1234} \cdot a_{R4} + c_{R123} \cdot a_{R3} + c_{R12} \cdot a_{R2} + c_{R1} \cdot a_{R1} \\ J_{R2,2} &= c_{R1234} \cdot a_{R4} + c_{R123} \cdot a_{R3} + c_{R12} \cdot a_{R2} \\ J_{R2,3} &= c_{R1234} \cdot a_{R4} + c_{R123} \cdot a_{R3} \\ J_{R2,4} &= c_{R1234} \cdot a_{R4} \end{aligned}$$

In the same way the Jacobian of the left arm (J_L) can be found by replacing all "R" subscripts by "L" in (3).

Let F_R and F_L be the amount of forces exerted to the object by the right and left arms, respectively. Their magnitudes can be related to joint torques as

$$\tau_R = J_R^T \cdot F_R \quad \text{and} \quad \tau_L = J_L^T \cdot F_L \quad (4)$$

for the right and left arms, respectively. The above equations can be combined as

$$\tau_a = J^T \cdot F \quad (5)$$

in which $\tau_a = [\tau_R \ \tau_L]^T$ and $F = [F_R \ F_L]^T$ are column vectors containing the joint torques and the tip point forces for both arms, respectively. The Jacobian matrix relating these torques and forces is $J = \begin{bmatrix} J_R & 0 \\ 0 & J_L \end{bmatrix}$ in which 0 is a matrix of proper dimensions with all its members zero.

At the object level, the vector of the exerted force is F_a with equal dimensions as F_R and F_L that is the dimension of task-space (i.e., $m = 2$). By simple static equilibrium condition of the object, one may show that

$$F_a = F_R + F_L. \quad (6)$$

This can be written as

$$F_a = G \cdot F \quad (7)$$

in which

$$G = \begin{bmatrix} 1 & 0 & 1 & 0 \\ 0 & 1 & 0 & 1 \end{bmatrix} \quad (8)$$

is called the grasp matrix.

As a simple relation between the force exerted by the manipulator (F_a) and the joint torques vector (τ_a), one may write an equation like (4) as

$$\tau_a = J_a^T \cdot F_a \quad (9)$$

in which J_a may be defined as the *apparent Jacobian* of the whole manipulator. Substituting (7) in (9) yields

$$\tau_a = J_a^T \cdot G \cdot F \quad (10)$$

Comparing (10) to (5) reveals that

$$J^T = J_a^T \cdot G \quad (11)$$

This implies

$$J_a^T = J^T \cdot G^\dagger \quad (12)$$

with G^\dagger being the pseudo-inverse of the grasp matrix, defined as

$$G^\dagger = G^T \cdot (G \cdot G^T)^{-1} \quad (13)$$

Note that $(G \cdot G^T)$ is a 2×2 full-rank matrix and thus can be inverted.

4. DACL Manipulator Optimal Configuration

As described in Section 3, the DACL manipulator considered here, consists of two 4 degrees-of-freedom arms. Thus the total DOF of the manipulator is 8, but as the arms cooperate in their common workspace, two constraints are imposed on each arm to maintain its tip-point on the object – a specified planar point. This makes four constraint Eqs. (1) and (2) as described earlier. The robot is to handle the point object using these two arms. For this purpose, the joint values are calculated so as to maximize the robot’s ability to exert force in a desired direction $[dx \ dy]^T$ when their tip-points correspond to the location of object (P_x, P_y) . This is done while the effort of the robot is kept constant (i.e., the joint forces are bounded). As discussed in ref. [17], the classical hypothesis is to assume that

$$\tau_a^T \cdot \tau_a = 1, \quad (14)$$

i.e., to keep the Euclidian norm of the joint torque vector as unity. Substituting (9) in (14) gives

$$F_a^T \cdot J_a \cdot J_a^T \cdot F_a = 1. \quad (15)$$

This relation changes the hypersphere of the joint forces into a hyperellipsoid that is called the *resistivity ellipsoid*. We want to optimize the exerted force, F_a , to its maximum

magnitude in the specified direction. Thus we write it as

$$F_a = f \cdot \begin{bmatrix} dx \\ dy \end{bmatrix} = f \cdot \hat{F}_a, \quad (16)$$

in which f is the magnitude of F_a and \hat{F}_a is a vector of unit length on its direction.

Substituting (16) in (14) yields

$$f^2 \cdot (\hat{F}_a^T \cdot J_a \cdot J_a^T \cdot \hat{F}_a) = 1 \quad (17)$$

In order to maximize f , it is suitable to minimize the term in the parentheses. So the optimization criterion is

$$\text{Minimize : } (\hat{F}_a^T \cdot J_a \cdot J_a^T \cdot \hat{F}_a) \quad (18)$$

For this, some constraints must be considered, four of which are (1) and (2).

Collision of the arm links with one another must be avoided considering the fact that the DACL manipulator is planar. To this end, each arm link is considered a segment and geometrical formulations are derived to prevent segments from crossing each other. If the coordinates of start and end points of a segment, namely (x_{1R}, y_{1R}) and (x_{2R}, y_{2R}) , are known, the equation of the line passing through these two points is

$$y - y_{1R} = \frac{y_{2R} - y_{1R}}{x_{2R} - x_{1R}}(x - x_{1R}) \quad (19)$$

This is also the geometrical expression of the direction of the segment between (x_{1R}, y_{1R}) and (x_{2R}, y_{2R}) . Similarly, the line passing through points (x_{1L}, y_{1L}) and (x_{2L}, y_{2L}) is

$$y - y_{1L} = \frac{y_{2L} - y_{1L}}{x_{2L} - x_{1L}}(x - x_{1L}). \quad (20)$$

Next is to find the point of collision of the two lines (i.e., the segment directions), and then obtain the condition that causes the intersection point (x_i, y_i) to be out of at least one of the segment lines (see Fig. 5). The distances between the intersection point and the middle points of the segments are called d_R and d_L , for right and left arms, respectively. Thus the condition of collision prevention between the two segments is

$$d_R \geq 0.5 a_R \quad \text{or} \quad d_L \geq 0.5 a_L \quad (21)$$

where a_R and a_L are the lengths of the right and left arms, respectively.

But in order to impose the constraint of Eq. (21) over the optimization problem, we must combine both equations and come up with one equation to be considered along with other constraints.

To do that, we introduce two new parameters

$$C_R = d_R - 0.5 \cdot a_R, \quad C_L = d_L - 0.5 \cdot a_L \quad (22)$$

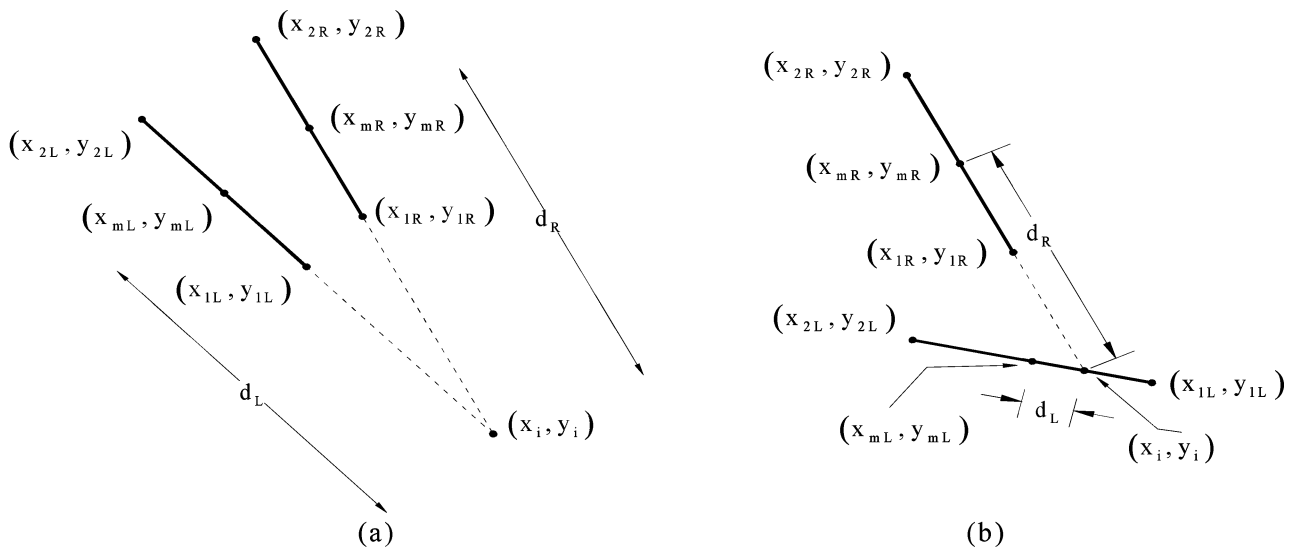


Fig. 5. Two positions for non-intersecting segments.

Thus the condition of (21) becomes

$$0 \leq C_R \text{ or } 0 \leq C_L \tag{23}$$

And these conditions may be combined as one constraint

$$(C_R - |C_R|).(C_L - |C_L|) = 0 \tag{24}$$

Equation (24) implies that C_R , C_L or both must have non-negative values. That is to say, collision of the two links is not allowed except on the joints – the latter means that they are cam-locked joints.

5. Numerical Results

As an example for our optimization problem, we have considered a DACL manipulator with all the links having unit length. That is

$$a_{iR} = a_{iL} = 1 \text{ for } i = 1, 2, 3, 4 \tag{25}$$

Using the method of sequential quadratic programming, which is a nonlinear optimization method accepting nonlinear equality and inequality constraints, we can find the best manipulator configuration that applies the largest possible amount of force in the direction desired. The object is assumed to be at the position

$$\begin{aligned} P_x &= 0.2 \\ P_y &= 3.5 \end{aligned} \tag{26}$$

and the desired direction

$$\begin{aligned} d_x &= 1 \\ d_y &= -0.1 \end{aligned} \tag{27}$$

Upon solving the problem, the angles for the optimal configuration are found to be (in degrees)

$$\theta_{1R} = 64.59, \quad \theta_{2R} = 4.89, \quad \theta_{3R} = 11.27,$$

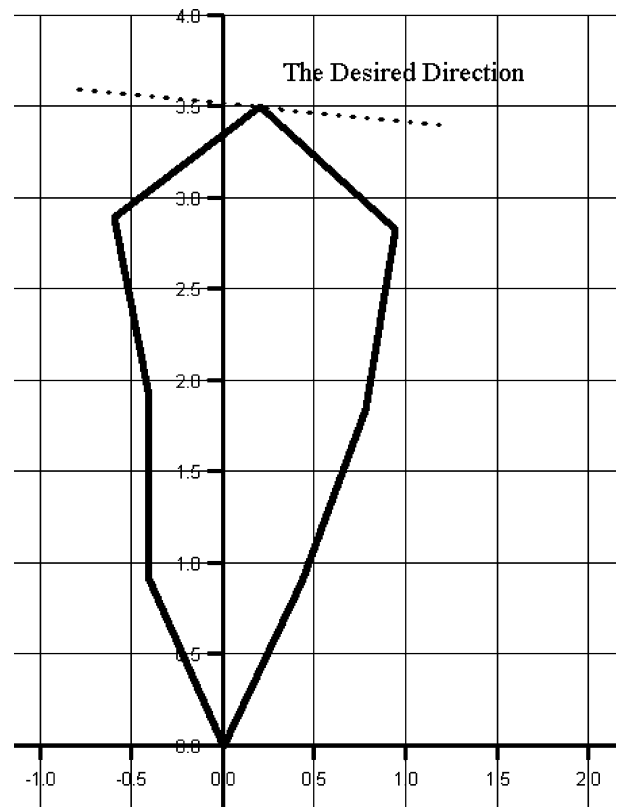


Fig. 6. The configuration of the dual-arm cam-lock manipulator for the numerical example with no locked joints.

$$\begin{aligned} \theta_{4R} &= 56.93, \quad \theta_{1L} = 114.11, \quad \theta_{2L} = -24.05, \\ \theta_{3L} &= 10.69, \quad \theta_{4L} = -63.54 \end{aligned} \tag{28}$$

where the applicable force at the robot's tip with this configuration was $f = 0.3012$. Figure 6 shows the configuration of the DACL manipulator for this case. Furthermore, if first joints are locked into each other and the problem is solved with new conditions, the angles for the

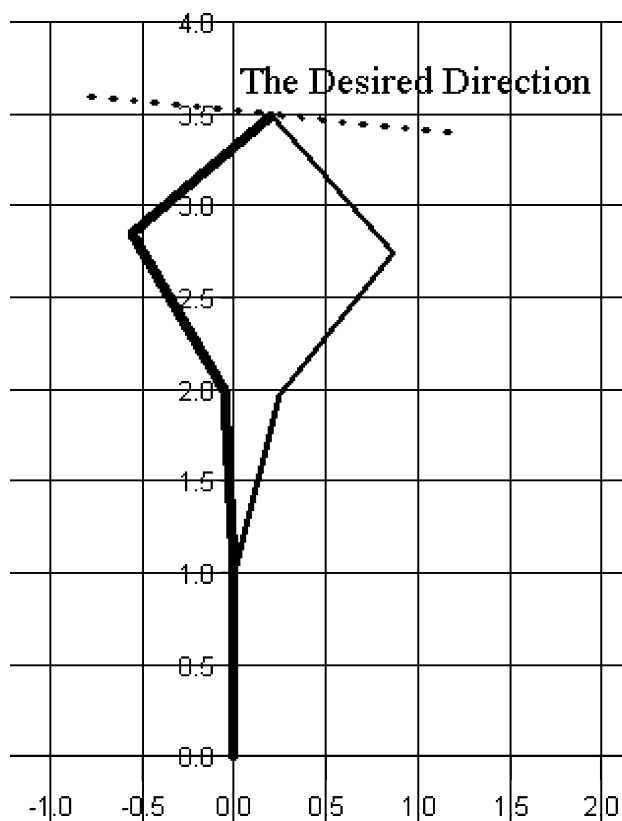


Fig. 7. The configuration of the dual-arm cam-lock manipulator for the numerical example with first joints locked in each other.

optimal configuration are found to be (in degrees)

$$\begin{aligned} \theta_{1R} &= 90.00, & \theta_{2R} &= -13.78, & \theta_{3R} &= -24.91, \\ \theta_{4R} &= 80.25, & \theta_{1L} &= 90.00, & \theta_{2L} &= 3.17, \\ \theta_{3L} &= 27.59, & \theta_{4L} &= -80.80 \end{aligned} \quad (29)$$

where the applicable force with this configuration was $f = 0.3061$. For this case, the robot configuration is shown in Fig. 7. As a result, it is obvious that the locked configuration is more suitable for exerting the maximum force to the point object in the desired direction.

6. Conclusion

The kinetostatic relations of the DACL robot have been developed. The manipulator is redundant and a suitable criterion has been introduced to find the optimal configuration. When the robot tip holds an object at a specified point, it is aimed to maximize the force that the robot can apply in a desired direction. For that purpose, the concept of force manipulability ellipsoid is utilized to define the function to

be optimized. In addition the constraints of the problem are obtained to maintain the tip points of the right and left arms on the object. To avoid collision between the links of the arms, suitable formulations are developed and imposed upon the optimization problem as equality constraints.

References

1. J. K. Salisbury and J. J. Craig, "Articulated hands: Force control and kinematic issues," *Int. J. Robot. Res.* **1**(1), 4–17 (1982).
2. J. Y. S. Luh and Y. F. Zheng, "Constrained relations between two coordinated industrial robots for motion control," *Int. J. Robot. Res.* **6**(3), 60–70 (1987).
3. P. Dauchez and M. Uchiyama, "Kinematic Formulation for Two Force-controlled Cooperating Robots," *Proceedings of the 3rd International Conference of Advanced Robotics*, Versailles, France (1987) pp. 457–467.
4. Y. Nakamura, K. Nagai and T. Yoshikawa, "Mechanics of Coordinative Manipulation by Multiple Robotic Mechanisms," *Proceedings of the IEEE International Conference on Robotics Automation*, Raleigh, NC (1987) pp. 991–998.
5. T. Yoshikawa, "Manipulability of robotic mechanisms," *Int. J. Robot. Res.* **4**(1), 3–9 (1985).
6. S. Chiu, "Task compatibility of manipulator postures," *Int. J. Robot. Res.* **7**(5), 13–21 (1988).
7. S. Lee, "Dual redundant arm configuration optimization with task-oriented dual arm manipulability," *IEEE Trans. Robot. Autom.* **5**(1), 78–97 (1989).
8. T. Kokkinis and B. Paden, "Kinetostatic Performance Limits of Cooperating Robot Manipulators Using Force-velocity Polytopes," *Proceedings of ASME Winter Annual Meeting-Robotics Research*, San Francisco, (1989) pp. 151–155.
9. P. Chiacchio, S. Chiaverini, L. Saiavicco and B. Siciliano, "Global task space manipulability ellipsoids for multiple-arm systems," *IEEE Trans. Robot. Autom.* **7**(5), 678–685 (1991).
10. C. Y. Kim and Y. S. Yoon, "Task space dynamic analysis or multi-arm robot using isotropic velocity and acceleration radii," *Robotica* **15**, pp. 319–329 (1997).
11. S. Krut, O. Company and F. Pierrot, "Velocity performance indices for parallel mechanisms with actuation redundancy," *Robotica* **22**, 129–139 (2004).
12. V. C. Klema and A. J. Laub, "The singular value decomposition: Its computation and some applications," *IEEE Trans. Autom. Control.* **AC-25**(2), 164–176 (1980).
13. J. G. Lau and M. A. Arteaga, "Dynamic model and simulation of cooperative robots: A case study," *Robotica* **23**, 615–624 (2005).
14. A. Meghdari, "Conceptual design and dynamics modeling of a cooperative dual-arm cam-lock manipulator," *Robotica* **14**(4), 301–309 (1996).
15. A. Meghdari, "The Cooperative Dual-arm Cam-Lock Manipulator," *Proceedings Of the IEEE International Conference on Robotics for Automation*, San Diego, CA, USA (1994) vol. 2, pp. 1279–1285.
16. A. Meghdari, "Conceptual Design and Characteristics of a Dual-arm Cam-Lock Manipulator," *Proceedings Of the ASCE SPACE-94 International Conference on Robotics for Challenging Environments*, Albuquerque, N.M., USA (1994) pp. 140–148.
17. J. P. Merlet, *Parallel Robots*, 2nd ed. (Springer, 2006).